Computers & Geosciences 55 (2013) 84–95

Contents lists available at SciVerse ScienceDirect

Computers & Geosciences

journal homepage: www.elsevier.com/locate/cageo

History matching of petroleum reservoir models by the Ensemble Kalman Filter and parameterization methods

Leila Heidari [a,b,*], Véronique Gervais [a], Mickaële Le Ravalec [a], Hans Wackernagel [b]

[a] IFP Energies nouvelles, 1-4, Avenue de Bois Préau, 92852 Rueil-Malmaison, France
[b] Geostatistics Group, Centre de Géosciences, MINES ParisTech, 35, Rue Saint Honoré, 77300 Fontainebleau, France

ARTICLE INFO

Article history:
Received 9 November 2011
Received in revised form
4 June 2012
Accepted 6 June 2012
Available online 23 June 2012

Keywords:
Ensemble Kalman Filter
EnKF
History matching
Parameterization
Gradual deformation method
Pilot point method

ABSTRACT

The Ensemble Kalman Filter (EnKF) has been successfully applied in petroleum engineering during the past few years to constrain reservoir models to production or seismic data. This sequential assimilation method provides a set of updated static variables (porosity, permeability) and dynamic variables (pressure, saturation) at each assimilation time. However, several limitations can be pointed out. In particular, the method does not prevent petrophysical realizations from departing from prior information. In addition, petrophysical properties can reach extreme (non-physical) values. In this work, we propose to combine the EnKF with two parameterization methods designed to preserve second-order statistical properties: pilot points and gradual deformation. The aim is to prevent the departure of the constrained petrophysical property distributions from prior information. Over/under estimations should also be avoided. The two algorithms are applied to a synthetic case. Several parameter configurations are investigated in order to identify solutions improving the performance of the method.

1. Introduction

The Ensemble Kalman Filter (Evensen, 1994) is a sequential assimilation method adapted to non linear dynamic problems. An ensemble of model realizations is used to represent the uncertainties in the model at hand. The model is propagated through time according to a dynamic system and, whenever measurements are available, new model estimates are computed following a variance minimization scheme (Evensen, 2007). This technique has been widely used in different fields of science such as oceanography (Haugen and Evensen, 2002), meteorology (Evensen and van Leeuwen, 1996), hydrogeology (Margulis et al., 2002) and petroleum engineering.

In petroleum applications, the model under consideration is the reservoir model. The state of this model changes with time because of fluid displacements. According to governing flow equations (Aziz and Settari, 1979), the reservoir state is characterized at each time by two sets of variables populating every grid block of the numerical reservoir model: on one hand, the *static variables* such as petrophysical properties (porosity, permeability), and, on the other hand, the *dynamic variables* that include pressures and fluid saturations. History matching then consists in perturbing the static variables in order to reproduce as best as possible the data collected during the life of the reservoir: production data at wells or seismic data for instance. The initial petrophysical property realizations are generated with respect to a prior geostatistical model deduced from geological data. It is characterized by a mean, a variance and a variogram, which describes the spatial variability of the properties. A correct definition of this model is crucial for the success of the history matching process. This is valid for variational history matching techniques, but also for EnKF since the updated models are linear combinations of the initial models. Several papers in the literature highlight the need for an appropriate initial ensemble to ensure a good match.

Other characteristics of the EnKF can impede its performance for history matching: the finite size of the ensemble, the Gaussian distribution assumption for the static and dynamic variables or the nonlinearity of the relation between measurements and variables. In particular, they can lead to extreme, nonphysical values for petrophysical properties (see Heidari et al. (2011) for instance). Indeed, the method does not prevent realizations from departing from prior information, yet playing an important role in the history matching process.

Let us note that other techniques have been investigated to quantify uncertainty in history-matching problems. One can refer for instance to Oliver et al. (2001), Dostert et al. (2006) or Romary (2009). A detailed review on reservoir history matching techniques can be found in Oliver and Chen (2011).

In this paper, we aim to constrain petrophysical realizations to honor prior information all along the assimilation process in order to avoid over/under estimation. The main idea is to combine the

* Corresponding author. Now at: With Total, Pau.
E-mail address: heidari.leila@gmail.com (L. Heidari).

0098-3004/$ - see front matter © 2012 Elsevier Ltd. All rights reserved.
http://dx.doi.org/10.1016/j.cageo.2012.06.006

EnKF with parameterization techniques designed for perturbing realizations while preserving their spatial variability. More precisely, the EnKF is applied to a set of parameters used to perturb an ensemble of fixed background realizations. The resulting ensemble of realizations evolves through assimilations and is used to perform fluid flow simulations. The parameterization techniques considered here are the pilot point method (de Marsily et al., 1984) and the gradual deformation method (Hu, 2000). However, the proposed approach can be extended to other techniques. For gradual deformation, parameters are weights used to combine realizations from the background ensemble. For pilot points, EnKF is used to update values of petrophysical properties at selected locations of the reservoir. The perturbed values are then propagated to the background realizations by kriging.

The proposed algorithms are described in Section 2 and applied to a synthetic reservoir in Section 3. For both parameterization techniques, various parameter configurations are studied. The choice of pilot point locations is crucial for the performance of the history-matching process. For gradual deformation, we investigate the size of the background ensemble. Local deformations are also considered, in an attempt to provide more flexibility.

2. Combining EnKF with parameterization methods

The general combination algorithm is described in Section 2.1. Its specific implementation for pilot points and gradual deformation is given in Sections 2.2 and 2.3, respectively.

2.1. General algorithm

The basics of the algorithm are presented in Fig. 1. Three ensembles are considered:

- a "background" ensemble of realizations for each petrophysical property of interest,
- an ensemble of parameters,
- a "simulation" ensemble with the petrophysical property realizations obtained when applying each set of parameters to the background ensemble.

The members of the background ensemble are generated according to prior information. At each assimilation time, the members of the simulation ensemble are forecasted in time. The resulting dynamic states are then constrained to production data in the EnKF update jointly with the parameters.

The algorithm, which can be directly extended to any number of petrophysical properties, is the following:

1. Generate M realizations $Z_k, k=1,...,M$ of the petrophysical property of interest (porosity, permeability…) using the prior information: they form the background ensemble.
2. Select P perturbation parameters and generate N initial sets of values for these parameters $\theta_i^{a,0}=(\theta_{i,1}^{a,0},...,\theta_{i,P}^{a,0}),\quad i=1...N$. They will be considered as static variables in the assimilation process.
3. Then, for each new assimilation time $t^n, n>0$,

a. apply the parameterization technique to the background ensemble using successively the N sets of parameter values $\theta_i^{a,n-1},\quad i=1...N$. This results in N realizations of the property of interest $Y_i^{n-1}=f(\theta_i^{a,n-1},Z_1,...,Z_M)$, $i=1...N$, defining the simulation ensemble.

b. compute the forecast from time t^{n-1} to time t^n for each member Y_i^{n-1} of the simulation ensemble. This provides a set of forecasted dynamic variables $S_i^{f,n},\quad i=1...N$ and production responses at wells $D_i^{f,n},\quad i=1...N$.

c. apply the analysis step of EnKF to the vector $(\theta_i^{a,n-1},S_i^{f,n},D_i^{f,n})_{i=1...N}$. The resulting updated vector $(\theta_i^{a,n},S_i^{a,n},D_i^{a,n})_{i=1...N}$ is used as the initial state for the forecast at the next assimilation. A detailed description of the EnKF analysis step is given in Evensen (2007).

When considering several petrophysical properties, perturbation parameters should be chosen for each of them. Note that, in the traditional application of EnKF for history matching, the parameters and simulation ensembles are the same: the analysis step is applied to the petrophysical properties at all grid blocks (see also Fig. 1).

2.2. EnKF and pilot points

The pilot point method was first considered as an estimation method in the work by de Marsily et al. (1984) about the interpretation of interference test data. The purpose was to generate a smooth permeability model applying kriging to permeability values assigned to some points called *pilot points*. This method was further extended to condition permeability realizations to pressure data (RamaRao et al., 1995) by minimizing an objective (cost) function.

In order to understand the principle of the pilot point method, let us consider an unconditional realization y of some petrophysical property and n pilot points. y can be conditioned to new values at pilot point locations by conditional simulation through

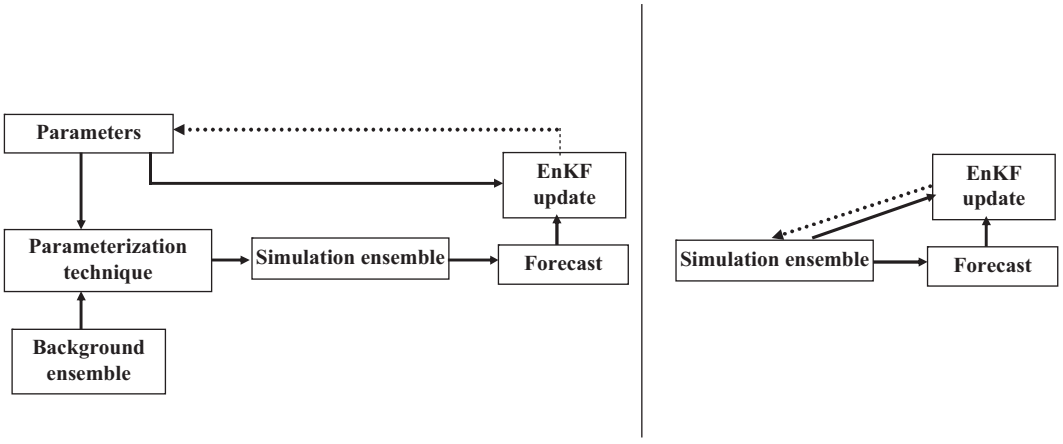

Fig. 1. Overview of the algorithm combining the EnKF and parameterization methods (left). Comparison with traditional EnKF (right).

kriging (Chilès and Delfiner, 1999):

$$y_c(u) = y_K^{pp}(u) + [y(u) - y_K(u)]$$

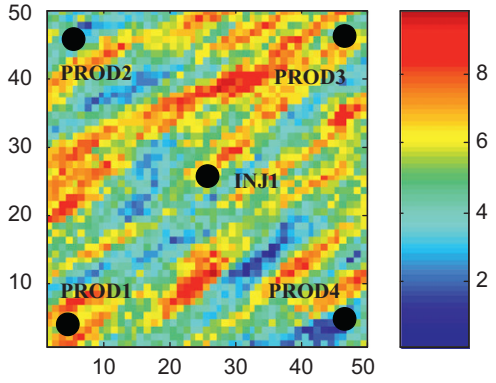

Fig. 2. Reference ln(Kh) field.

u indicates location. $y_K^{pp}(u)$ is the kriging estimate built from the new values imposed to the n pilot points, and $y_K(u)$ is the kriging estimate computed from the values of the unconditional y realization at pilot point locations.

The pilot point method can be used as a parameterization technique in history matching processes: the values of the petrophysical properties at pilot points are considered as independent uncertain parameters. Depending on the location of pilot points and on the values attributed at these points, the spatial variability of the perturbed realization may depart from the prior information. Among possible solutions, one can impose a minimal distance between pilot point locations and a confidence interval on the values. More details on the use of pilot points for history matching can be found in RamaRao et al. (1995), Gomez-Hernandez et al. (1997), de Marsily et al. (2000) and Oliver and Chen (2011).

The use of pilot points in the algorithm described above simply consists in updating petrophysical properties at pilot point locations using EnKF. The background ensemble contains $M=N$ realizations of the petrophysical property of interest. These realizations are conditioned to P pilot points on the basis of kriging to generate the simulation ensemble.

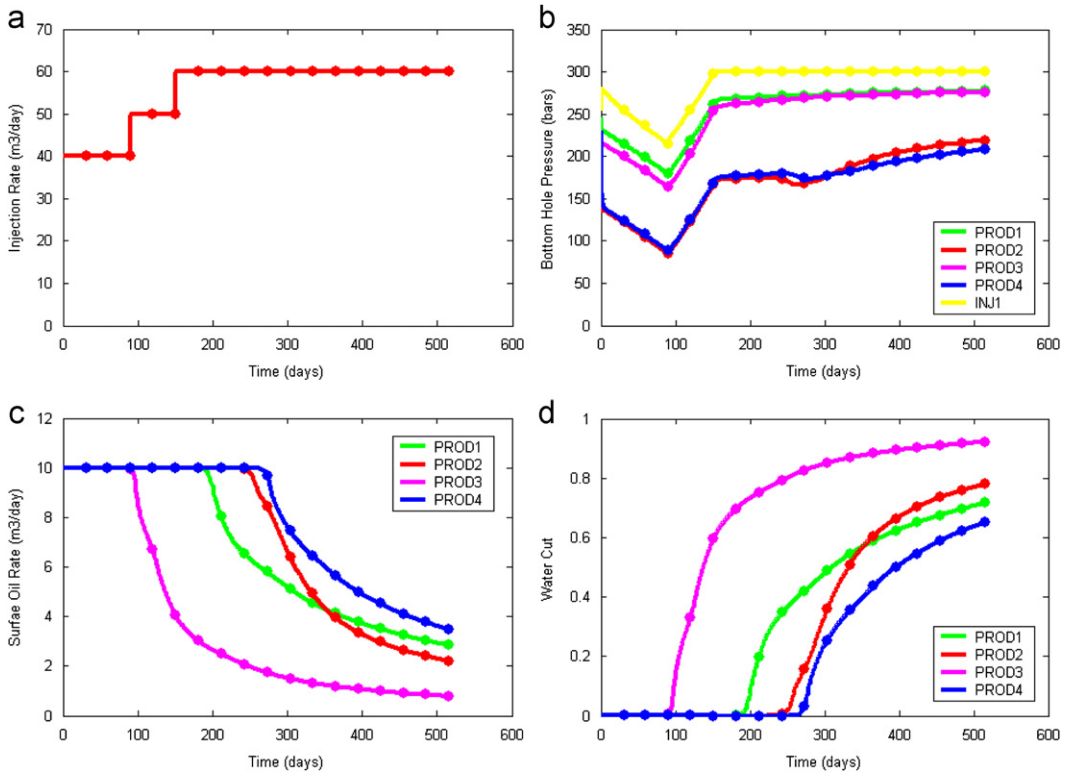

Fig. 3. (a) Maximum injection rate planning (b) Reference bottom hole pressure (c) Reference surface oil rate (d) Reference water cut. Solid dots indicate data used in the assimilation process.

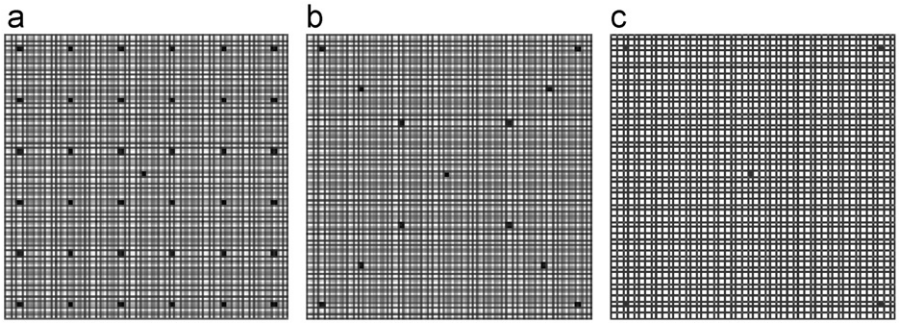

Fig. 4. Configurations for pilot point locations (black dots). (a) Configuration 2, (b) Configuration 3 and (c) Configuration 4.

2.3. EnKF and gradual deformation

The gradual deformation method was first introduced by Hu (2000). Let us consider two independent Gaussian random functions, Y_1 and Y_2 with the same mean m and covariance C. Hu proposed an adequate weighted combination of these functions, which results in a Gaussian random function Y satisfying the same statistical properties. For any parameter θ, Y is defined as

$$Y-m=(Y_1-m)\cos(\pi\theta)+(Y_2-m)\sin(\pi\theta) \quad (1)$$

θ is the gradual deformation parameter. The above formula is periodic in θ, with a range of -1 to $+1$. For $\theta=0$, Y is the same as Y_1; for $\theta=0.5$, Y is the same as Y_2. Continuous perturbations of θ result in continuous changes in Y. The same formulation can be applied to any two realizations y_1 and y_2 of Y_1 and Y_2 (respectively) to yield a realization y.

Eq. (1) can be extended to any number of realizations. Let us consider M independent Gaussian random functions $Y_1,...,Y_M$ with mean m and covariance C. Then, with any set of deformation parameters $\theta_1,...,\theta_{M-1}$,

$$Y-m=\prod_{i=1}^{M-1}(Y_1-m)\cos(\pi\theta_i)+\sum_{i=1}^{M-1}\sin(\pi\theta_i)\prod_{j=i+1}^{M-1}\cos(\pi\theta_j)(Y_{i+1}-m) \quad (2)$$

defines a Gaussian random function Y with mean m and covariance C.

The gradual deformation can be applied to Gaussian white noise realizations. This can be used in particular to combine gradual deformation to Gaussian and non-Gaussian simulation algorithms such as the FFT-MA algorithm proposed by Le Ravalec et al. (2000), sequential simulations or object-based Boolean simulations.

In order to get more flexibility, different deformation parameter values can be assigned to non overlapping regions of the reservoir grid. In this case, the gradual deformation is said to be "local" (Hu, 2000).

Let us now consider the integration of gradual deformation in the algorithm of Section 2.1. The perturbation parameters are the gradual deformation parameters, so that necessarily $P=M-1$. The background ensemble contains M realizations of the petrophysical property of interest or eventually Gaussian white noise realizations. In both cases, the combination in (Eq. (2)) is applied to the members of this ensemble. Gaussian white noise realizations are then transformed into petrophysical realizations with mean m and covariance C using a geostatistical algorithm. In the following, the FFT-MA method will be considered.

The initial set of deformation parameters $\theta_k^{a,0}=(\theta_{k,1}^{a,0},...,\theta_{k,P}^{a,0})$, $k=1...N$ is generated randomly from a uniform distribution before being submitted to a normal score transformation (as EnKF requires Gaussian distributions).

Finally, the algorithm can be easily extended to local gradual deformations when considering the Gaussian white noise realizations as the background ensemble. In such a case, a set of deformation parameters is defined per region. The members of the background ensemble are then combined in each grid cell according to (Eq. (2)), considering the value of the deformation parameters associated to the region the grid cell belongs to.

3. Numerical experiment

In this section we propose to apply the previous methods to a synthetic case study. It consists of a two dimensional, two phase flow (water and oil), water flooding synthetic reservoir. The uncertain parameter is the horizontal permeability field. The other properties such as the porosity, the relative permeability curves, *etc.*, are assumed to be known. The aim of the experiment

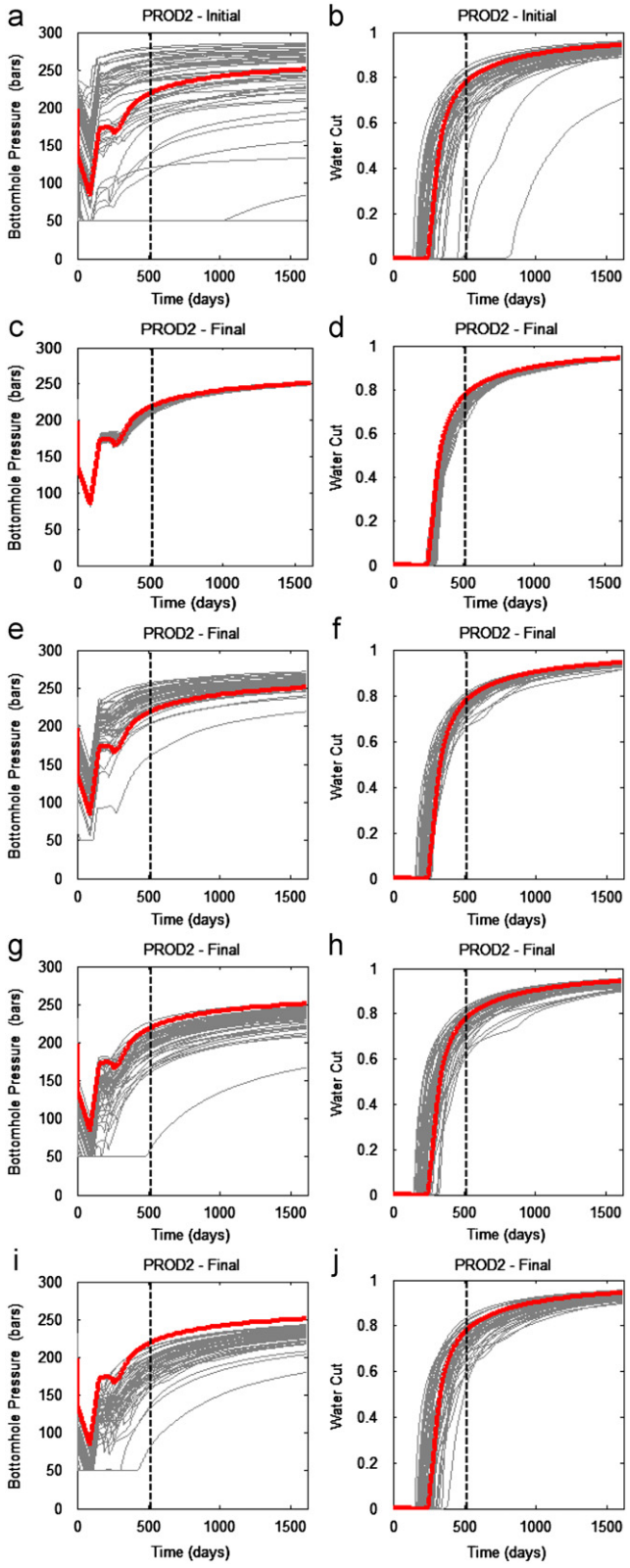

Fig. 5. Bottom hole pressure (left) and water cut (right) simulated at well PROD2 with the initial ensemble (first row) and the final ensemble obtained for configurations 1 to 4. Reference data are plotted in red. The black dashed vertical line separates the history-matching period (0–516 day) from the forecasting period (517–1612 day). (a) Initial ensemble, (b) Initial ensemble, (c) Final ensemble - Configuration 1, (d) Final ensemble - Configuration 1, (e) Final ensemble - Configuration 2, (f) Final ensemble - Configuration 2, (g) Final ensemble - Configuration 3, (h) Final ensemble - Configuration 3, (i) Final ensemble - Configuration 4 and (j) Final ensemble - Configuration 4. (For interpretation of the references to color in this figure legend, the reader is referred to the web version of this article.)

is then to generate a set of permeability fields constrained to production data using the algorithms proposed above.

3.1. Case study description

The numerical model for the 2D case study is built over a 50×50 grid. The dimensions of grid blocks are 10 m × 10 m. For simplicity, the porosity is equal to 0.18 everywhere. See Fig. 2 for the reference realization of the logarithm of the horizontal permeability *Kh*. It was generated using the Fast-Fourier Transform-Moving Average (FFT-MA) algorithm (Le Ravalec et al., 2000) with a mean of 5, a variance of 2.5 and an anisotropic spherical variogram. The main anisotropy direction is defined by an angle of 30° with respect to the *X*-axis. The correlation lengths, *i.e.* the practical ranges of the variogram, are 200 and 40 m.

Five vertical wells are located in the field: one water injector (INJ1) in the center and one producer in each corner (named PROD1 to PROD4, clockwise). The top depth of the reservoir is 2200 m and the initial reservoir pressure is 250 bars. We consider here a two phase (water and oil) black-oil model. Relative permeability curves follow a Corey law (Corey, 1977) with an exponent of 2. The residual water saturation is set to 0.15 and the residual oil saturation to 0.2. Water and oil compressibility equal 0.10×10^{-4} and 0.10×10^{-3} bar^{-1}, respectively. The corresponding densities are 1.05 and 0.9 g/cm^3.

The production schedule is defined over 4.5 years. All producers are imposed a 10 m^3/day rate. The flow rate constraint is changed to a bottom hole pressure (BHP) control when BHP drops below 50 bars. The primary constraint for the injection well is the maximum water injection rate, initially set to 40 m^3/day. It is changed to 50 m^3/day and 60 m^3/day after 90 and 151 day of production, respectively (see Fig 3(a)). The secondary constraint for this well is the allowed maximum injection pressure, which is set to 300 bars.

The bottom hole pressure (BHP), surface oil rate (SOR) and water cut (WCT) simulated at the wells for the reference permeability field are considered as reference production data in the following. All fluid-flow simulations are performed using the reservoir simulator PumaFlow™ (see for instance Gratien et al. (2007)).

Table 1
Effect of pilot points: final RMS_1 error for each type of production response normalized to the value obtained with EnKF.

	RMS for bottom hole pressure	RMS for surface oil rate	RMS for water cut
Configuration 1 (EnKF—2500 points)	1	1	1
Configuration 2 (37 points)	7.61	3.41	3.39
Configuration 3 (13 points)	7.48	3.68	3.66
Configuration 4 (5 points)	10.7	3.65	3.58

For the assimilation process, the reference permeability field is assumed to be unknown. The aim of the experiment is thus to obtain a set of permeability realizations constrained to the production data. The history matching interval consists of the first 17 months (516 day), with data assimilation at the end of each month. The corresponding reference data are plotted in Fig. 3(b)–(d). The period from days 517–1612 is used to assess the forecast capabilities of the constrained models.

The measurement errors are assumed to be independent and Gaussian distributed with a standard deviation set to 5% of the measured values. An initial ensemble of $N=50$ sets is generated for the P parameter values. The state vector updated with the EnKF analysis is the following:

- Parameters $\theta_{i,1},\ldots,\theta_{i,P}$ (static variables)
- Pressure $P_{1,i},\ldots,P_{2500,i}$ and water saturation $S_{1,i},\ldots,S_{2500,i}$ in all grid cells (dynamic variables)
- Bottom hole pressures $BHP_{i,k}, k=1\ldots5$ in all wells, surface oil rate $SOR_{i,k}, k=1\ldots4$ and water cut $WCT_{i,k}, k=1\ldots4$ at producers.

In the following, the quality of the results will be assessed using in particular the RMS error on the reference production data and permeability field. This value estimates the departure of the simulated production data or permeability realizations from the reference values as

$$RMS_1 = \sqrt{\frac{1}{N}\sum_{i=1}^{N}\frac{1}{N_t}\sum_{j=1}^{N_t}\frac{1}{N_{data}^{t_j}}\sum_{k=1}^{N_{data}^{t_j}}\left(d_{obs}^{k}(t_j)-d_i^k(t_j)\right)^2} \quad \text{(production data)} \qquad (3)$$

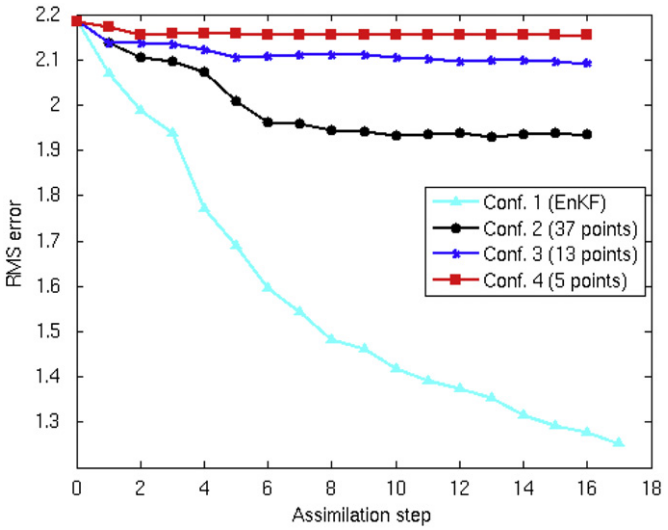

Fig. 7. RMS_2 error on the ln(Kh) realization during the assimilation process.

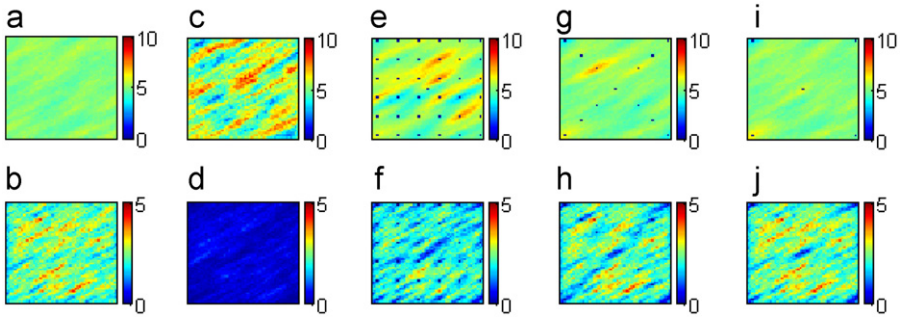

Fig. 6. Mean (first row) and variance (second row) of the ln(Kh) realizations in the initial ensemble (left) and the final ensembles obtained with configurations 1–4. (a) Initial, (b) Initial, (c) Final – Configuration 1, (d) Final – Configuration 1, (e) Final – Configuration 2, (f) Final – Configuration 2, (g) Final – Configuration 3, (h) Final – Configuration 3, (i) Final – Configuration 4 and (j) Final – Configuration 4.

and

$$RMS_2 = \sqrt{\frac{1}{N}\sum_{i=1}^{N}\frac{1}{N_{grid}}\sum_{p=1}^{N_{grid}}(\ln(Kh)_p^i - \ln(Kh)_p^{ref})^2} \quad \text{(permeability field)} \qquad (4)$$

N is the ensemble size, N_{grid} the number of grid blocks, N_t the number of data assimilation time steps, $N_{data}^{t_j}$ the number of production data collected at time t_j. i is the ensemble member index, p the grid block index, j the time index and k the production

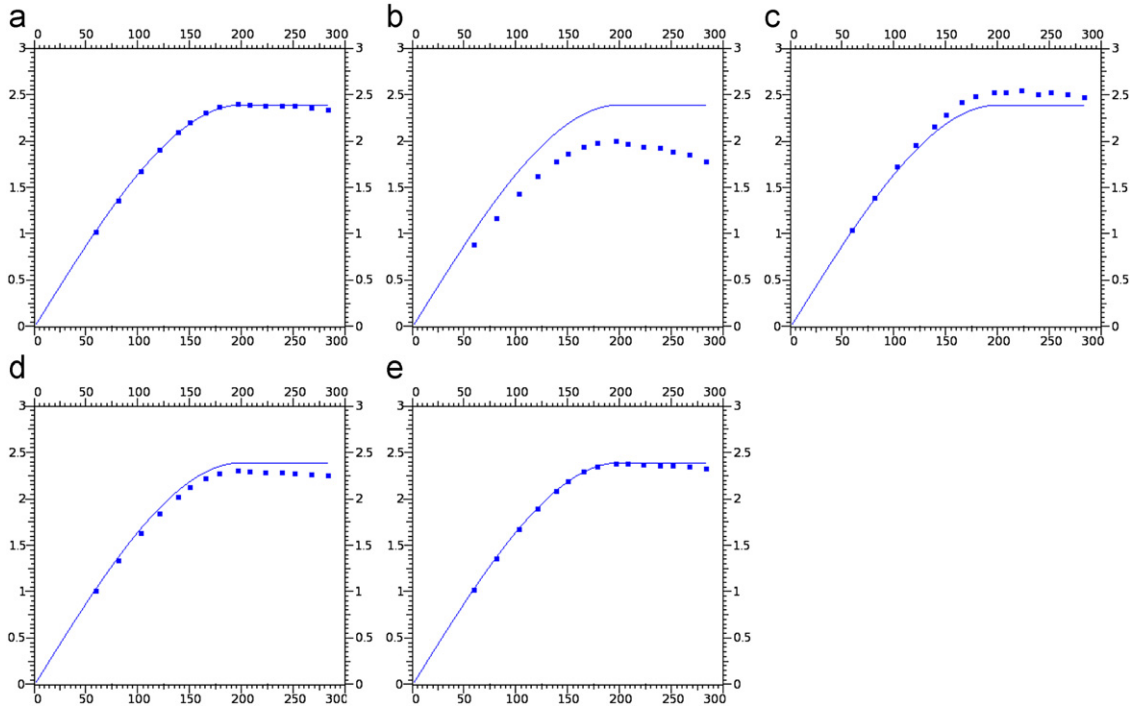

Fig. 8. Experimental variogram computed in the main anisotropy direction on all the realizations of the initial ensemble and updated ensembles considering the four configurations (blue dots). The blue lines correspond to a spherical variogram with the range of the reference model (200 m) and a variance of 2.4. (a) Initial ensemble, (b) Configuration 1 (2500 points – EnKF), (c) Configuration 2 (37 points), (d) Configuration 3 (13 points) and (e) Configuration 4 (5 points). (For interpretation of the references to color in this figure legend, the reader is referred to the web version of this article.)

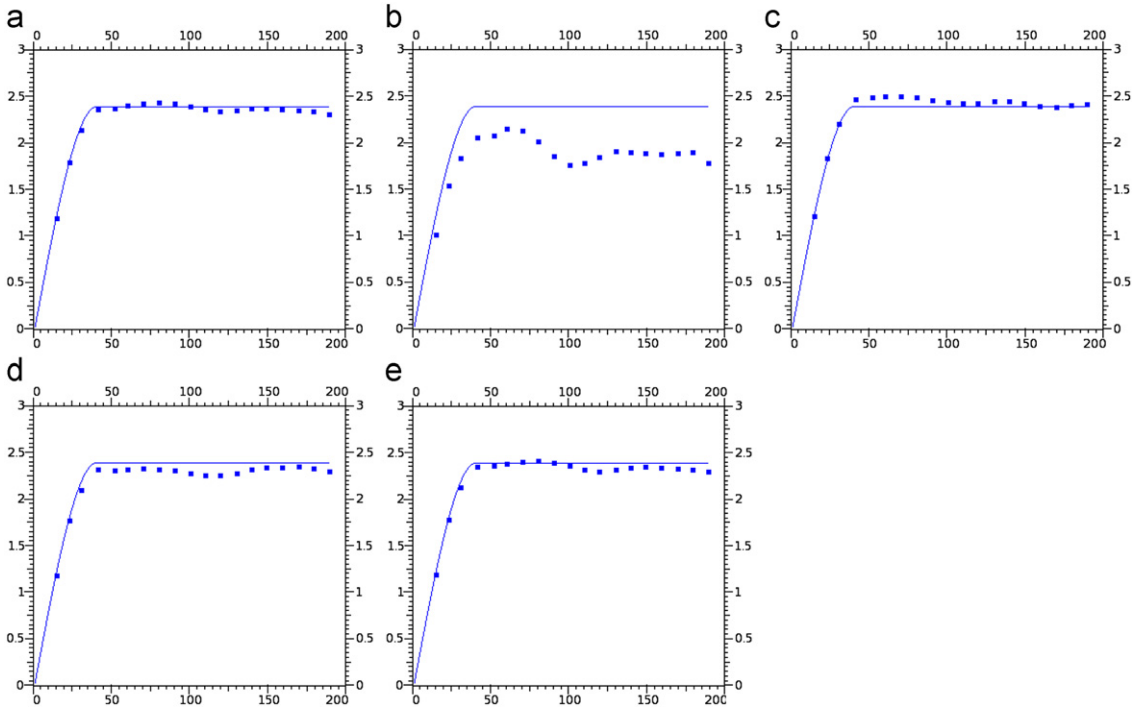

Fig. 9. Experimental variogram computed in the second anisotropy direction on all the realizations of the initial ensemble and updated ensembles considering the four configurations (blue dots). The blue lines correspond to a spherical variogram with the range of the reference model (40 m) and a variance of 2.4. (a) Initial ensemble, (b) Configuration 1(2500 points - EnKF), (c) Configuration 2(37 points), (d) Configuration 3(13 points) and (e) Configuration 4(5 points). (For interpretation of the references to color in this figure legend, the reader is referred to the web version of this article.)

response index. $d_{obs}^{k}(t_j)$ is the kth observed data at time t_j and $d_i^k(t_j)$ is the kth data simulated at time t_j with the ith ensemble member. Finally, $\ln(Kh)_p^{ref}$ denotes the reference petrophysical property $\ln(Kh)$ in grid block p.

3.2. ENKF and pilot points

When considering the combination of EnKF with the pilot point method as described in Section 2.1, the nature of static parameters is the same as in traditional EnKF. Using one pilot point per grid cell appears equivalent to EnKF since kriging is not applied in this case. The main issue here is the choice of pilot point locations, which is crucial for the efficiency of the history matching process.

Four configurations are considered in this study. The first one consists of one pilot point per grid block and is thus equivalent to EnKF. For the others, points are removed progressively, trying to keep the locations influencing production responses while increasing the distance between points to better preserve spatial variability. In the second configuration (Fig. 4(a)), 37 pilot points are considered: the injector location plus a regular gridding including producers. The entire reservoir is then almost covered. 13 pilot points are considered in the third configuration (Fig. 4(b)). They are located at wells and at almost even intervals between the

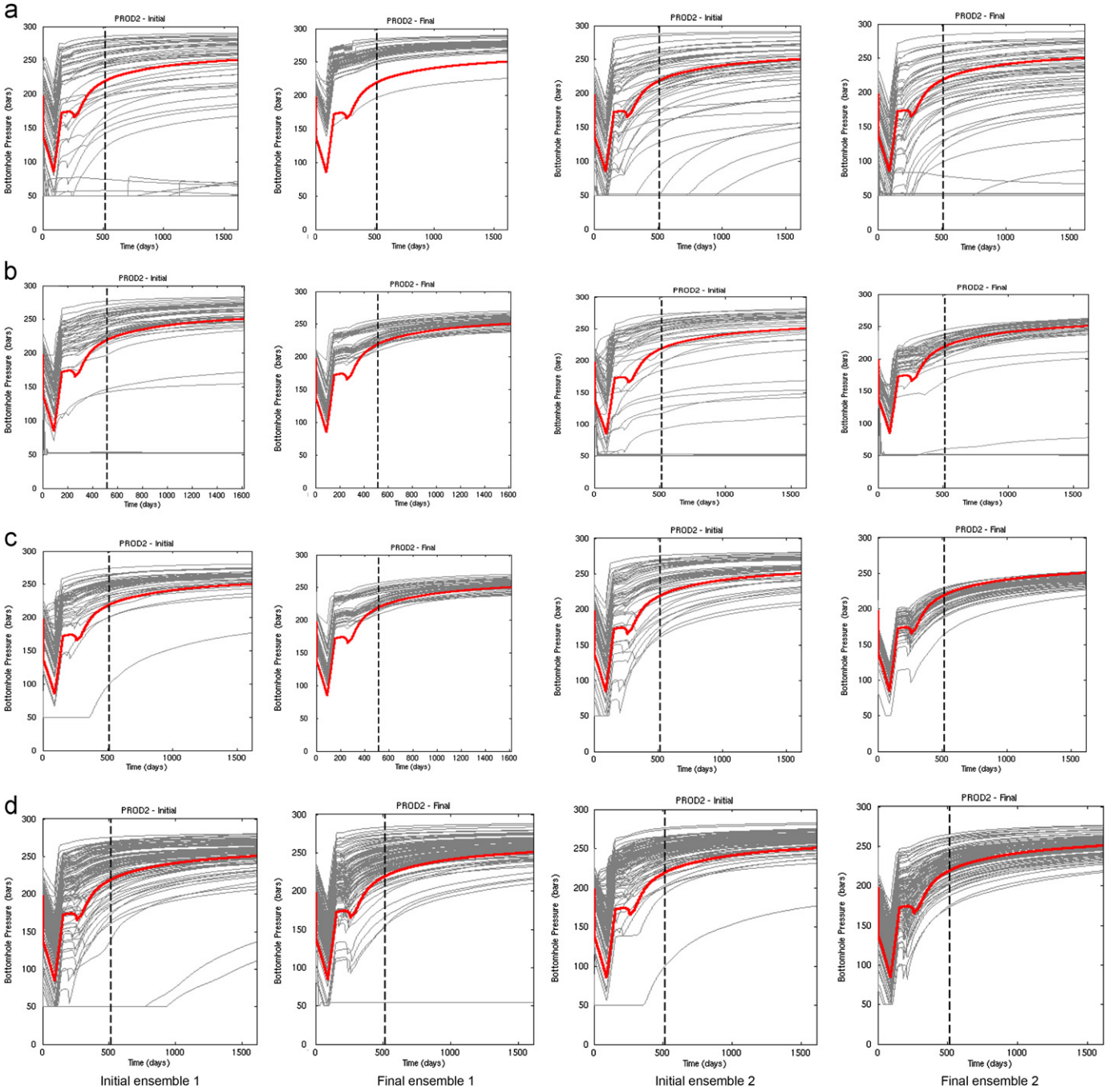

Fig. 10. Bottom hole pressure simulated at well PROD2 with the initial ensembles (columns 1 and 3) and the corresponding final ensembles (columns 2 and 4) obtained applying the EnKF to the gradual deformation parameters and $N=50$ or 100, $M=100$, 1000 or 2500. Reference data are plotted in red. The black dashed vertical line separates the history-matching period (0–516 day) from the forecasting period (517–1612 day). (a) N=50, M=100, (b) N=50, M=1000, (c) N=50, M=2500 and (d) N=100, M=2500. (For interpretation of the references to color in this figure legend, the reader is referred to the web version of this article.).

injector and the producers. With this setting, we try to capture heterogeneities in the flow direction. Finally, well locations only are considered in the last configuration (Fig. 4(c)).

A background ensemble of 50 models is generated using the FFT-MA algorithm with the same statistical properties as the reference model. The values of these realizations at pilot point locations form the 50 members of the initial parameters ensemble. The background and initial simulation ensembles are thus identical.

As can be seen in Fig. 5(a)–(b) production responses simulated at well PROD2 with the initial ensemble members can differ strongly from the reference data (red curve). Performing the assimilation enables to get rid of outliers and to reduce the

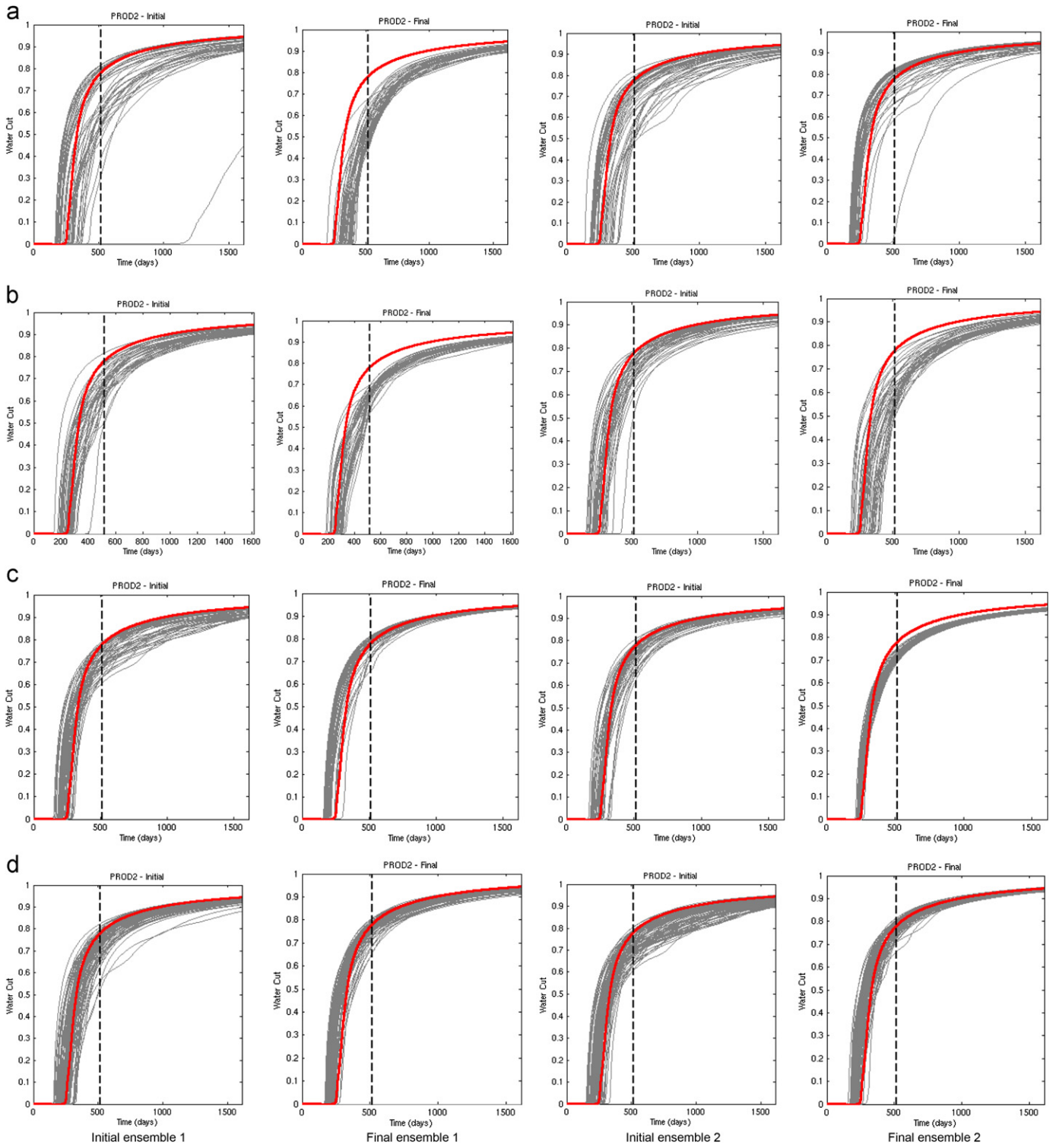

Fig. 11. Water cut simulated at well PROD2 with the initial ensembles (columns 1 and 3) and the corresponding final ensembles (columns 2 and 4) obtained applying the EnKF to the gradual deformation parameters and $N=50$ or 100, $M=100$, 1000 or 2500. Reference data are plotted in red. The black dashed vertical line separates the history matching period (0–516 day) from the forecasting period (517–1612 day). (a) N=50, M=100, (b) N=50, M=1000, (c) N=50, M=2500 and (d) N=100, M=2500. (For interpretation of the references to color in this figure legend, the reader is referred to the web version of this article.)

spread within responses (Fig. 5(c)–(j)). However, a degradation of the match and predictions is observed from configurations 1 to 4.

The RMS error on the production data (Eq. (3)) computed for the final ensembles described above is given in Table 1. A value is computed per production response type (bottom hole pressure, surface oil rate and water csut). Also, values computed for configuration 1 (EnKF) are used to normalize the results. One can observe that the RMS values tend to decrease when the number of pilot points increases.

The final mean and variance are represented in Fig. 6 for each configuration. From configuration 1 to 4, we can observe a smoother mean and a higher variance, which mainly reduces near pilot points. More precisely, the mean permeability obtained with the first configuration (traditional EnKF, Fig. 6(c)–(d)) reproduces some features of the reference field (Fig. 2). However, the variance within the ensemble is very low, and it seems to have almost converged towards a model different from the reference one. On the contrary, the mean permeability obtained with configuration 4 is homogeneous and variance has only decreased near wells (pilot points). For the two other configurations, we can observe some heterogeneities of the mean while variance remains at a satisfactory level. Fig. 7 shows the evolution of the RMS error on ln(Kh) during assimilations (Eq. (4)). Its value decreases during the assimilation process: the higher the number of pilot points, the larger the decrease in RMS. However, the variance among the ensemble members decreases at the same time and reaches a very low value for EnKF although the RMS error is not null.

Thus, the EnKF method provides here very similar realizations with a good match on the data, but different from the reference one. Pilot points utilization preserves more heterogeneity among

Table 2
Effect of gradual deformation: average RMS_1 error on the two ensembles considered for each configuration.

	RMS for bottom hole pressure	RMS for surface oil rate	RMS for water cut
N=50, M=100	5.471	0.3111	0.0308
N=50, M=1000	5.7744	0.2881	0.0283
N=50, M=2500	4.228	0.2443	0.0245
N=100, M=1000	4.477	0.2154	0.0215
N=100, M=2500	3.176	0.2028	0.0203
5 zones, N=50, M=100	3.0879	0.2295	0.0229
100 zones, N=50, M=100	1.3428	0.2326	0.0232

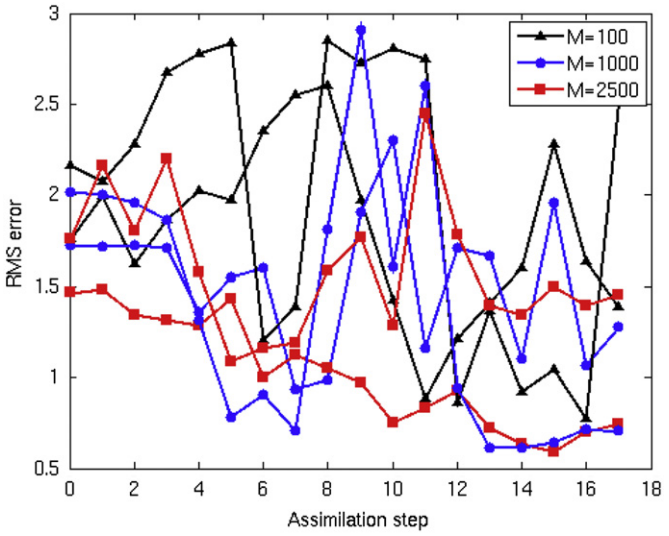

Fig. 13. RMS_2 error on the ln(Kh) reference field during the assimilation processes.

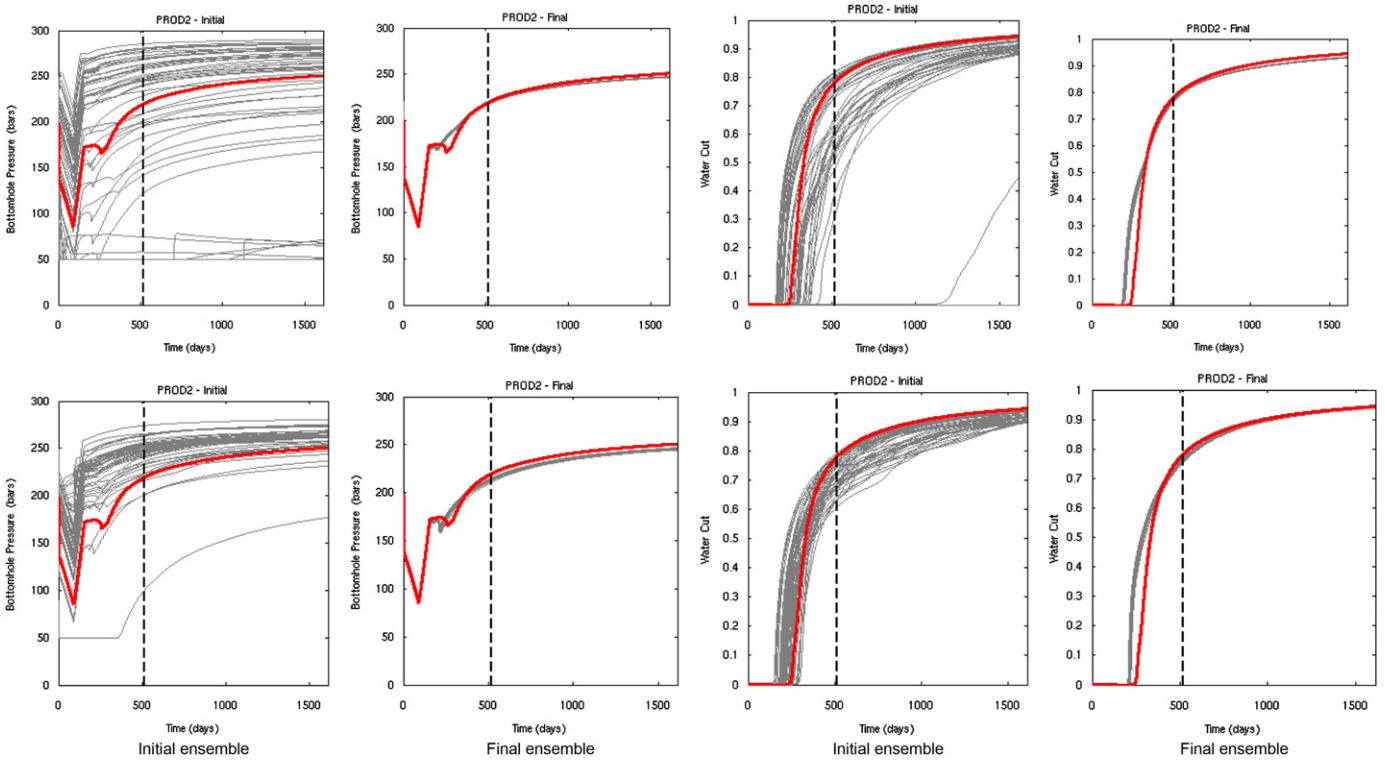

Fig. 12. Bottom hole pressure (left) and water cut (right) simulated at well PROD2 with the initial ensembles (columns 1 and 3) and the corresponding final ensembles (columns 2 and 4) obtained applying the traditional EnKF to the initial simulation ensembles, $N=50$ and $M=100$ and 2500. Reference data are plotted in red. The black dashed vertical line separates the history matching period (0–516 day) from the forecasting period (517–1612 day). (For interpretation of the references to color in this figure legend, the reader is referred to the web version of this article.)

the members of the ensemble than traditional EnKF. Some models provide as good matching results as EnKF. Some others can still be improved.

Finally, the experimental variograms computed over the initial and updated ensembles are shown in Fig. 8 and Fig. 9 considering the main anisotropy direction and the orthogonal one. The blue

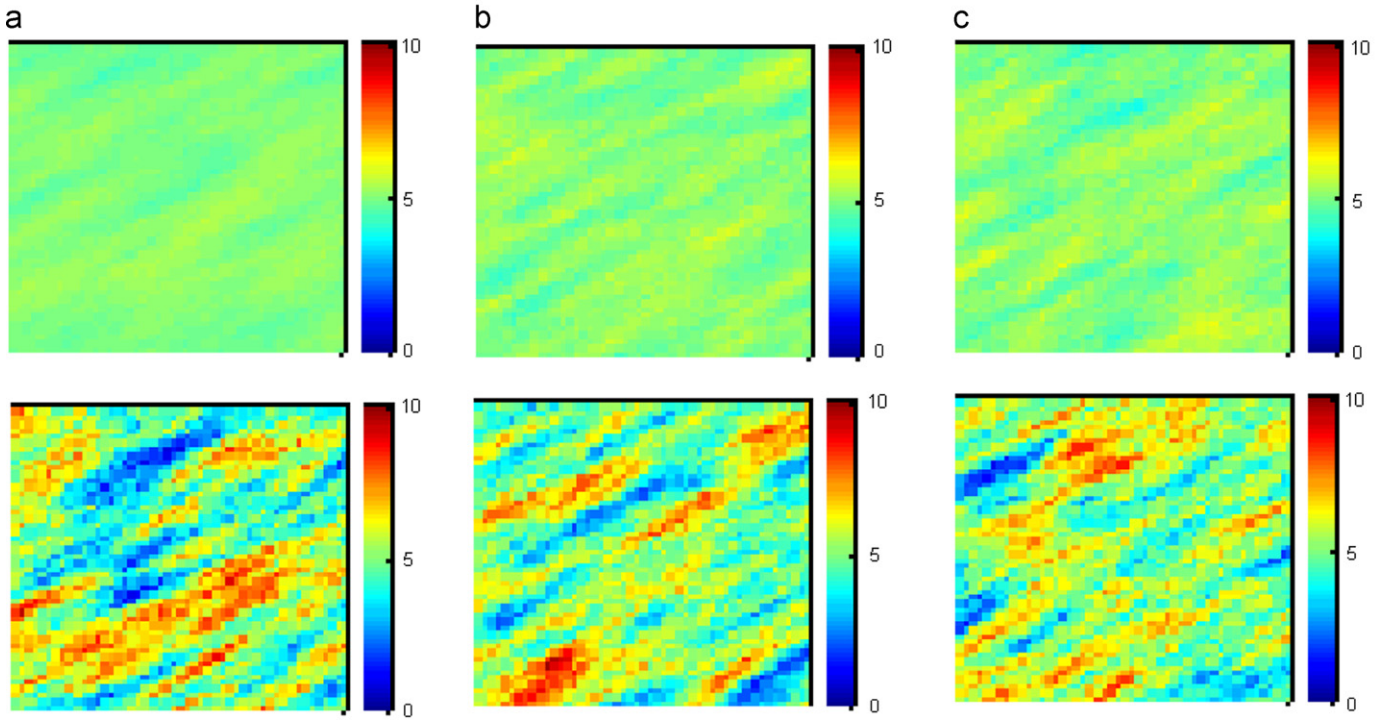

Fig. 14. Mean of the initial (top) and final (bottom) ln(Kh) realizations within ensembles obtained applying the EnKF to gradual deformation parameters and $M=100$, 1000 and 2500 ($N=50$). (a) $M=100$, (b) $M=1000$ and (c) $M=2500$

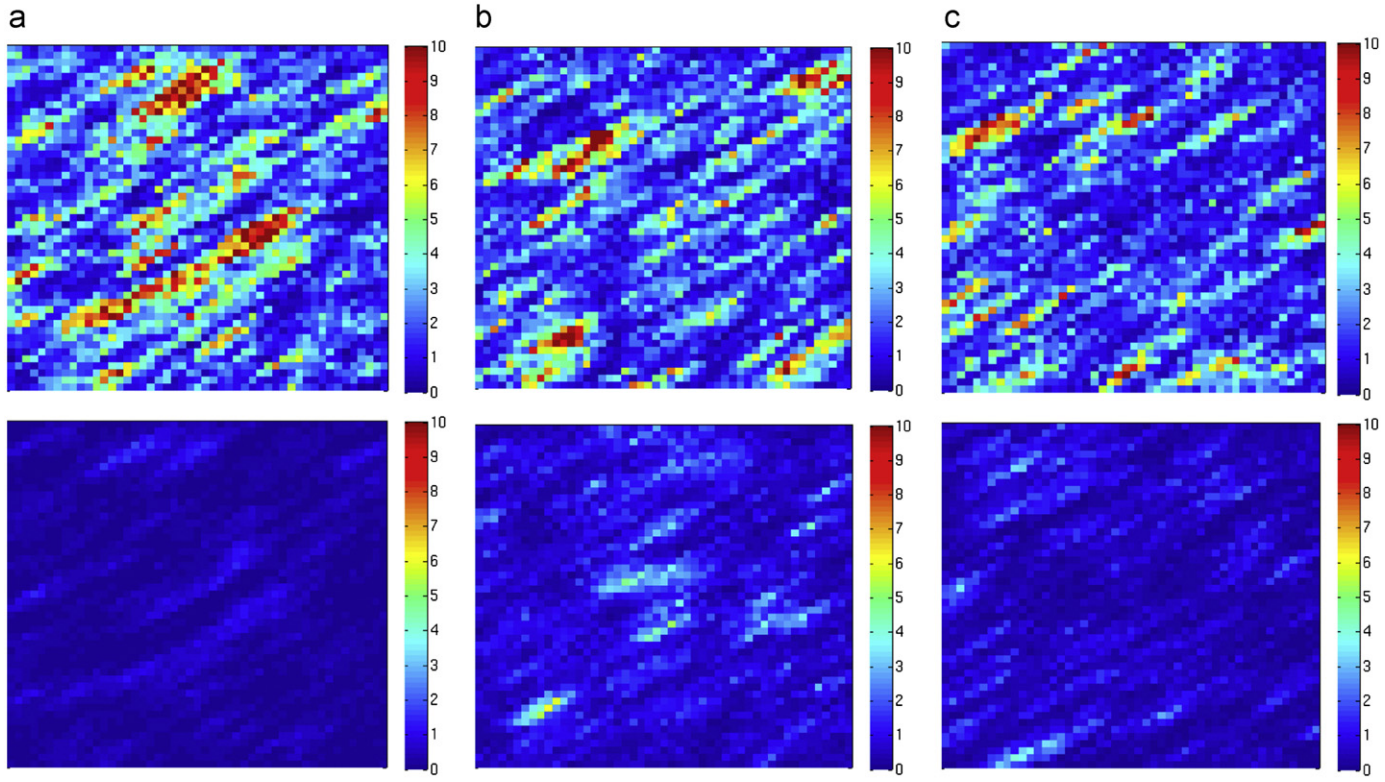

Fig. 15. Variance of the initial (top) and final (bottom) ln(Kh) realizations within ensembles obtained applying the EnKF to gradual deformation parameters and $M=100$, 1000 and 2500 ($N=50$). (a) M=100, (b) M=1000 and (c) M=2500.

lines correspond to a spherical variogram with the ranges of the reference model and a variance of 2.4. As can be seen, the variance computed on the initial ensemble is slightly lower than the theoretical one, equal to 2.5. This is probably due to the finite size of the ensemble and could be improved by selecting the initial models among a larger ensemble. The variograms computed for the ensembles updated with the proposed method remain close to the initial one. With EnKF, we observe that the variogram departs from the theoretical one. This may be due to spurious correlations introduced by the filter. The very low variance within the EnKF ensemble may also induce these results.

To conclude, it seems that considering the permeability values at some points only in the update step provides a higher variability among ensemble members. The quality of the match turns out to be strongly dependent on the pilot points location and number. As a general rule, points should be considered in regions influencing the production response. Then, it seems that the larger the number, the better the quality of predictions. An optimal configuration of pilot point location is thus required to obtain a good balance between variability preservation and production data match. This problem is case dependent and was already addressed for variational history matching. A review can be found in Oliver and Chen (2011) for instance.

3.3. EnKF and gradual deformation

In a first set of experiments, we consider background ensembles of Gaussian white noise realizations with increasing size: $M=100$, 1000 and 2500. These ensembles are transformed into simulation ensembles of $N=50$ permeability realizations using the FFT-MA algorithm and the same statistical properties as the ones characterizing the reference model.

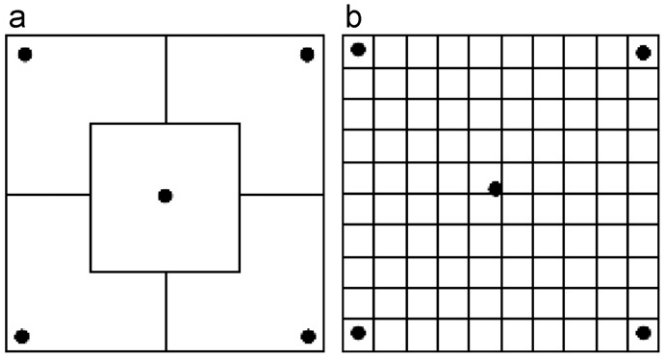

Fig. 16. Reservoir partitioning for local gradual deformation. (a) 5 zone configuration and (b) 100 zone configuration.

Two background ensembles were considered for each value of M. The bottom hole pressure and the water cut simulated over the whole production history in well PROD2 with the initial simulation ensembles and the final permeability fields for $M=100$, 1000 and 2500 are given in Fig. 10(a)–(c) and Fig. 11(a)–(c). As a general trend, we observe that the spread within the simulated responses is reduced. The match of production data seems better with $M=2500$ than $M=100$, what could be linked to the increasing size of the background ensemble, or equivalently the search space.

This trend is also visible on the average RMS error on the production data (Eq. (3)) computed for the final ensembles described above (Table 2): its value tends to decrease for an increasing size of the background ensemble.

With the present method, the permeability models of the initial simulation ensembles are obtained from the combination of the same Gaussian white noise realizations. They are thus correlated and the variance in many grid blocks can be quite low (see Fig. 15). This is probably one of the reasons why the method shows much sensitivity to the choice of the background ensemble and initial gradual deformation parameters. Also, the results obtained after assimilation with standard EnKF from the initial simulation ensembles are not so good (Fig. 12).

The evolution of the RMS error on the reference permeability field (Eq. 4) during the assimilation processes is given in Fig. 13. A global decreasing trend is observed, but quite chaotic. Fig. 14 and Fig. 15 represent the mean and variance of the initial and final $\ln(Kh)$ realizations obtained for some of the previous experiments. The mean value becomes more heterogeneous. The variance gets lower, but keeps a higher level than with EnKF.

The size of the simulation ensemble is an important factor for the quality of the results obtained with traditional EnKF. Therefore, in a second set of experiments, the size of the simulation ensemble was increased from 50 to 100. Again, we consider two background ensembles for $M=1000$ and $M=2500$. The bottom hole pressure and the water cut simulated over the whole production history in well PROD2 with the initial simulation ensembles and the final permeability fields are given in Fig. 10(d) and Fig. 11(d). The RMS results for the production response (Eq. (3)) are reported in Table 2. We can observe that the final average RMS error tends here to decrease for both an increasing size of the simulation ensemble and an increasing size of the background ensemble.

In the last set of experiments, we introduce local deformations to add more flexibility. Two simple configurations for reservoir

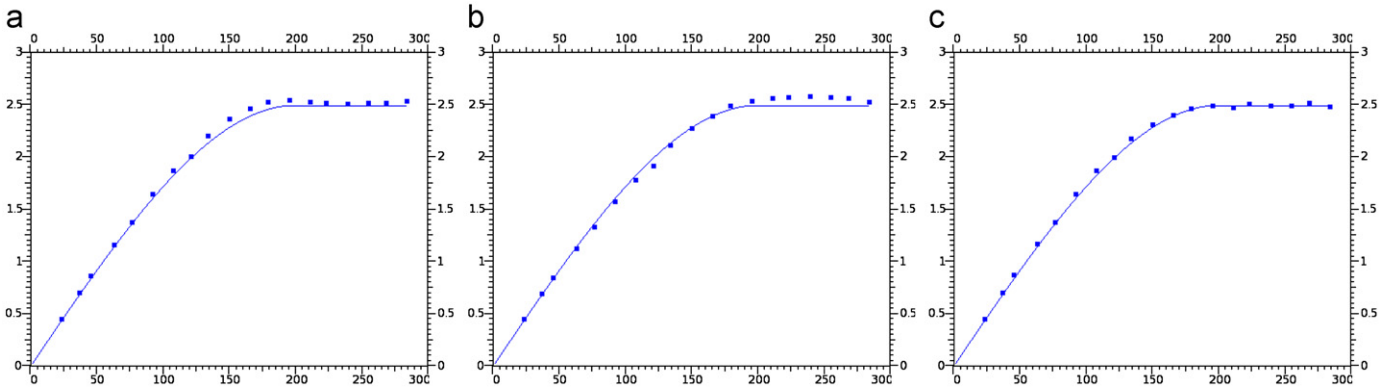

Fig. 17. Experimental variogram computed on all the realizations of the initial and updated ensembles with 5 and 100 zones in the main anisotropy direction (blue dots). The blue line corresponds to the theoretical variogram of the reference model. (a) 100 zones - initial ensemble, (b) 100 zones – final ensemble and (c) 5 zones – final ensemble. (For interpretation of the references to color in this figure legend, the reader is referred to the web version of this article.).

partitioning are set up, but more complex ones could also be envisaged. In the first one (Fig. 16, left), the grid is split into 5 non regular zones surrounding wells. The regions around producers are made up of 481 grid blocks. The middle one contains 576 grid blocks. In the second configuration (Fig. 16, right), the grid is divided into 100 squares of 5×5 grid blocks. The assimilation scenario is the same as before. A background ensemble with $M=100$ Gaussian white noise realizations is used to generate a simulation ensemble of $N=50$ ln(Kh) realizations.

RMS results for the production response (Eq. (3)) are reported in Table 2. Increasing the number of zones in the reservoir and consequently the size of the search space leads to a global decrease of the RMS error.

Finally, the experimental variogram in the main anisotropy direction computed over the initial and final simulation ensembles are displayed in Fig. 17. It remains very close to the theoretical variogram of the reference model (blue line).

To conclude, the results presented here for gradual deformation are of interest. Better results can be obtained considering a larger background ensemble, a larger simulation ensemble or local deformations. However, the method shows much sensitivity to the initial background ensemble and seems to lack stability in terms of quality of the results for a given configuration. Other ways to combine gradual deformation with EnKF may improve the results.

4. Conclusions

In this paper, we have proposed a technique to perform sequential assimilation with the EnKF combined to parameterizations of the petrophysical property realizations designed for preserving the prior two-order statistics. A set of parameters updated with the EnKF has been used to perturb a fixed background ensemble of realizations. These parameters can be gradual deformation parameters or values of petrophysical properties at pilot points.

The resulting algorithms were applied to a 2D synthetic case study. The performance of the algorithm combining the EnKF and the pilot point method strongly depends on the number and location of pilot points. Considering too few points will lack efficiency in terms of data match. However, ensemble members show less variability when increasing the number of points. A balance needs thus to be found between data match and variability preservation, and other configurations should be investigated. Finally, this technique could be very valuable for facies models and requires further tests on more complex case studies. For gradual deformation, results can be improved with an increased flexibility provided by larger background ensembles, larger simulation ensembles or local deformations. However, the quality of the results remains very sensitive to the initial background ensemble.

References

Aziz, K., Settari, A., 1979. Petroleum Reservoir Simulation. Applied Science, London.

Chilès, J.P., Delfiner, P., 1999. Geostatistics—Modeling Spatial Uncertainty. Wiley series in Probability and Statistics, New York, USA.

Corey, A.T., 1977. Mechanics of heterogeneous fluids in porous media. Water Resources Publications, Fort Collins, Coloradi.

de Marsily, G., Delhomme, J.P., Coudrain-Ribstein, A., Lavenue, A.M., 2000. Four decades of inverse problems in hydrogeology. Geophysical Society of America, Special paper 348.

de Marsily, G., Lavedan, G., Boucher, M., Fasanino, G., 1984. Interpretation of interference tests in a well field using geostatistical techniques to fit the permeability distribution in a reservoir model, Geostatistics for Natural Resources Characterization. Reidel, Dordrecht, pp. 831–849.

Dostert, P., Efendiev, Y., Hou, T.Y., Luo, W., 2006. Coarse-gradient Langevin algorithms for dynamic data integration and uncertainty quantification. Journal of Computational Physics 217 (1), 123–142.

Evensen, G., 1994. Sequential Data Assimilation with a nonlinear quasi-geostrophic model using Monte Carlo methods to forecast error statistics. Journal of Geophysical Resources 99 (10), 10143–10162.

Evensen, G., 2007. Data Assimilation: The Ensemble Kalman Filter. Springer Verlag, Berlin.

Evensen, G., van Leeuwen, P.J., 1996, Horizontal and vertical structure of the representer functions for sea structure measurements in a coastal circulation model, 30 2627–2635.

Gomez-Hernandez, J.J., Sahuquillo, A., Capilla, J.E., 1997. Stochastic simulation of transmissivity fields conditional to both transmissivity and piezometric data. 1. Theory. Journal of Hydrology 203, 162–174.

Gratien, J.M., Guignon, T., Magras, J.F., Quandalle, P.Ricois O., 2007. Scalability and load balancing problems in parallel reservoir simulation, SPE 106023. In: Proceedings of the SPE Reservoir Simulation Symposium, Houston, Texas, 26–28 February.

Haugen, V.E.J., Evensen, G., 2002. Assimilation of SLA and SST data into OGCM for the Indian Ocean. Ocean Dynamics 52, 133–151.

Heidari, L., Gervais, V., Le Ravalec, M., Wackernagel, H., 2011. History matching of reservoir models by ensemble Kalman filtering: the state of the art and a sensitivity study. In: Ma, Y.Z., La Pointe, P.R. (Eds.), Uncertainty Analysis and Reservoir Modeling: AAPG Memoir, 96; 2011 249–264..

Hu, L.-Y., 2000. Gradual deformation and iterative calibration of Gaussian-related stochastic models. Mathematical Geology 32 (1), 87–108.

Le Ravalec, M., Noetinger, B., Hu, L.Y., 2000. The FFT moving average (FFT-MA) generator: an efficient numerical method for generating and conditioning Gaussian simulation. Mathematical Geology 32 (6), 701–723.

Margulis, S.A., McLaughlin, D., Entekhabi, D., Dunne, S., 2002. Land data assimilation and estimation of soil moisture using measurements from the Southern Great Plains 1997 Field Experiment. Water Resources 38 (12), 35.1–35.18.

Oliver, D.S., Chen, Y., 2011. Recent progress on reservoir history matching: a review. Computational Geosciences 15 (1), 185–221.

Oliver, D.S., Reynolds, A.C., Bi, Z., Abacioglu, Y., 2001. Integration of production data into reservoir models. Petroleum Geoscience vol. 7, S65–S73.

RamaRao, B.S., La Venue, A.M., de Marsily, G., Marietta, G., 1995. Pilot point methodology for automated calibration of an ensemble of conditionally simulated transmissivity fields, 1. Theory and computational experiments. Water Resources Research 31 (3), 475–493.

Romary, T., 2009. Integrating production data under uncertainty by parallel interacting Markov chains on a reduced dimensional space. Computational Geosciences 13 (1), 103–122.